MOLECULAR PHYSICS, 1987, VOL. 60, NO. 3, 573–595

Phase equilibria of fluid interfaces and confined fluids

Non-local versus local density functionals

by P. TARAZONA
Departmento de Fisica del Estado Solido (UAM),
and Instituto de Fisica del Estado Solido (CSIC),
Facultad de Ciencias, Universidad Autonoma,
Madrid 28049, Spain

U. MARINI BETTOLO MARCONI and R. EVANS
H. H. Wills Physics Laboratory, University of Bristol,
Bristol BS8 1TL, England

(*Received 1 August 1984; accepted 1 October 1984*)

Phase transitions at fluid interfaces and in fluids confined in pores have been investigated by means of a density functional approach that treats attractive forces between fluid molecules in mean-field approximation and models repulsive forces by hard-spheres. Two types of approximation were employed for the hard-sphere free energy functional: (*a*) the well-known local density approximation (LDA) that omits short-ranged correlations and (*b*) a non-local smoothed density approximation (SDA) that includes such correlations and therefore accounts for the oscillations of the density profile near walls. Three different kinds of phase transition were considered: (i) *wetting transition*. The transition from partial to complete wetting at a single adsorbing wall is shifted to lower temperatures and tends to become first-order when the more-realistic SDA is employed. Comparison of the results suggests that the LDA overestimates the contact angle θ in a partial wetting situation. (ii) *capillary evaporation* of a fluid confined between two parallel hard walls. This transition, from dense 'liquid' to dilute 'gas', occurs in a supersaturated fluid ($p > p_{sat}$). The lines of capillary coexistence calculated in the LDA and SDA are rather close, suggesting that non-local effects are not especially important in this case. (iii) *capillary condensation* of fluids confined between two adsorbing walls or in a single cylindrical pore. For a partial wetting situation the condensation pressures $p(<p_{sat})$ obtained from the SDA are in remarkably good agreement with the macroscopic Laplace (or Kelvin) prediction for wall separations H or pore radii $R_c \gtrsim 5\sigma$; σ is a molecular diameter. While, because of different packing, the density profiles of the fluid differ considerably between slits and cylinders this has little effect on the coexistence line until H or $R_c \sim \sigma$. In contrast to the LDA the SDA describes two-dimensional-like liquid-gas coexistence for very narrow pores ($H < \sigma$) and temperatures below the two-dimensional critical temperature and this has ramifications for the existence of capillary critical points.

1. Introduction

Understanding the microscopic structure and the thermodynamic properties of fluid interfaces has become an increasingly popular goal for physicists and chemists. From a theorist's viewpoint interfacial problems are intrinsically more difficult than bulk problems because they necessarily involve spatially varying (singlet) densities of atoms or molecules and anisotropic correlation functions. Many interfaces of practical interest involve solids either in the form of a single planar substrate which can adsorb molecules from a bulk fluid or, in the case of porous material, as confining and adsorbing substrates. The solid substrate is often modelled by a structureless wall that is assumed to exert an external potential on the fluid molecules. Wall–fluid interfaces raise particular difficulties for theories of inhomogeneous fluids. It is well-known that the density profile of a liquid near a wall usually exhibits oscillations that are on the scale of a molecular diameter. Any attempt to describe such local ordering requires an adequate treatment of short-ranged correlations between molecules. Although the widely used closure approximations to the wall–particle Ornstein–Zernike equation (Percus–Yevick, Mean-Spherical Approximation, Hyper-Netted-Chain etc.) provide a rather good description of hard-sphere fluids near walls it has been shown that these approximations often fail totally when the forces between molecules in the fluid include attractive as well as repulsive contributions [1]. In particular they cannot accommodate two coexisting (liquid and gas) phases near the substrate [2]. This means that they cannot be employed as the basis for a theory of contact angle and wetting phenomena at a single wall–fluid interface [2]. It also means that such approximations are not appropriate for investigations of the phase equilibria of fluids confined in narrow pores. Given that much of the experimental interest in fluid interfaces is linked to phase transitions or critical behaviour of one type or another, a different class of theories which do accommodate coexisting phases has been developed and applied successfully to adsorption, wetting, and wetting transitions at both wall–fluid and fluid–fluid interfaces [3] and to the phase equilibria of fluids in pores [4, 5]. These theories are based on the density functional approach [6] in which one constructs a functional $\Omega_V[\rho]$ of the average singlet density $\rho(\mathbf{r})$ and minimizes this with respect to $\rho(\mathbf{r})$ to obtain the equilibrium density and thermodynamic properties. Correlation functions are obtained by performing further functional differentiation.

Most work on wetting problems [3] and almost all [7] work on confined fluids [4, 5] has employed a local approximation for the part of the Helmholtz free energy that arises from repulsive forces between fluid molecules. Whilst not doing any gross injustice to long-ranged correlations in the inhomogeneous fluid, thereby allowing for the growth of wetting layers, phase transitions, criticality, etc., a local density approximation makes a crude (delta function) approximation to the short-ranged part of the direct correlation function of the inhomogeneous fluid [8]. This ensures that local ordering at a wall–fluid interface cannot be described by a local density approximation. In this paper we are concerned with the effects of local ordering on the nature of the phase equilibria at a single wall–fluid interface and in fluids confined in slit-like and cylindrical pores. We enquire whether more sophisticated non-local density functionals, that incorporate a more realistic description of short-ranged correlations, predict phase transitions that are changed significantly from those obtained in local density approximation.

Three separate, but related, problems are investigated. The first concerns the effect of non-locality on the order and location (in temperature) of the wetting transition at a wall–gas interface. The second involves the phase equilibria of a fluid confined between two parallel hard walls. A phase transition from a dense 'liquid' configuration with wetting films of gas at the walls to a dilute 'gas' configuration occurs as the wall-separation H is reduced at a fixed chemical potential $\mu > \mu_{sat}$, its value at bulk coexistence. This phenomenon of capillary evaporation is studied in both non-local and local approximations. The third topic is the capillary condensation, at $\mu < \mu_{sat}$, of 'gases' to 'liquids' in narrow cylindrical and slit-like pores that exert attractive forces on the fluid molecules in addition to confining them. Although this phenomenon is relevant to the adsorption of gases in mesoporous and microporous solids it has been studied in detail only in the local density approximation [4, 5, 9, 10]. When the pore radius R_c or the wall-separation H is a few molecular diameters one might expect local ordering effects to play a crucial role in determining the phase equilibria, i.e. packing considerations should become very important. Since the earlier calculations did not include such effects it is of considerable interest to examine the consequences of incorporating non-locality for the location of the condensation lines and the capillary critical points. Indeed several of these issues were raised in discussion after papers [5, 10] at a recent Faraday Symposium. Our present results provide further response to this discussion and shed new insight into capillary condensation for fluids in very narrow pores and at low temperatures.

The density functional approach that is used in our calculations is based on a smoothed density approximation to $\mathscr{F}_{hs}[\rho]$, the free energy functional of a hard-sphere fluid. While this is closely related to the fine-grained 'generalized van der Waals theory' of Nordholm and co-workers [11, 7], the prescription for the smoothed density $\bar{\rho}(\mathbf{r})$ is obtained by recognizing that $\mathscr{F}_{hs}[\rho]$ is the generating functional for the hierarchy of hard-sphere direct correlation functions [12]. The actual version employed here is due to Tarazona [13] who showed that it gives an excellent account of the oscillatory profiles of hard-sphere fluids near hard walls. Attractive forces between fluid molecules are treated in mean-field approximation. Other procedures for constructing smoothed densities have been developed recently [14, 15]; these are probably of comparable accuracy but have not yet been applied to the variety of problems that are investigated here.

Our paper is arranged as follows: in § 2 we describe the density functional and its two dimensional limit. The latter is relevant for fluids confined in very narrow slits where two-dimensional-like ordering can occur. § 3 contains the results of our calculations for the three different interfacial problems mentioned above. We conclude in § 4 with some final remarks.

2. Theory

(*a*) *Description of density functionals*

We consider a one-component fluid in an external potential $V(\mathbf{r})$ at a temperature T and chemical potential μ. The equilibrium density $\rho(\mathbf{r})$ is given by minimizing the grand potential functional [6]

$$\Omega_V[\rho] = \mathscr{F}[\rho] + \int d^3\mathbf{r}\rho(\mathbf{r})(V(\mathbf{r}) - \mu) \tag{1}$$

where the intrinsic Helmholtz free energy functional $\mathscr{F}[\rho]$ contains contributions from fluid–fluid interactions as well as the ideal gas term. The minimum value of Ω_V is Ω, the grand potential of the system. Following earlier workers we divide, somewhat arbitrarily, $\mathscr{F}[\rho]$ into two parts: $\mathscr{F}[\rho] = \mathscr{F}_{\text{rep}}[\rho] + \mathscr{F}_{\text{att}}[\rho]$; the first represents the free energy arising from repulsive forces between molecules while the second represents the contribution from attractive forces. If the repulsive forces are modelled by hard-spheres and the attractive forces are treated in mean-field fashion we obtain the approximation

$$\mathscr{F}[\rho] = \mathscr{F}_{\text{hs}}[\rho] + \frac{1}{2}\iint d^3\mathbf{r}\, d^3\mathbf{r}'\rho(\mathbf{r})\rho(\mathbf{r}')\phi_{\text{att}}(|\mathbf{r} - \mathbf{r}'|) \tag{2}$$

where $\phi_{\text{att}}(\mathbf{r})$ is the attractive part of the pairwise potential between two molecules in the fluid. The hard-sphere free energy functional is not known exactly for the three-dimensional fluid so further approximations must be made. The simplest, and most often used is the local density approximation (LDA):

$$\mathscr{F}_{\text{hs}}[\rho] = \int d^3\mathbf{r} f_{\text{hs}}(\rho(\mathbf{r})), \tag{3}$$

where $f_{\text{hs}}(\rho)$ is the Helmholtz free energy density of a uniform hard-sphere fluid. This approximation was employed by Sullivan [16] and by many subsequent authors in studies of inhomogeneous fluids near walls or at fluid–fluid interfaces [3]. It is well-known that such a local approximation cannot describe the oscillatory density profiles that usually occur for liquids near walls. These oscillations are associated with short-ranged correlations in the fluid which are absent in a local theory. The simplest ansatz for $\mathscr{F}_{\text{hs}}[\rho]$ that incorporates short-ranged correlations is based on a smoothed or coarse-grained density $\bar{\rho}(\mathbf{r})$. This density, which is a non-local functional of $\rho(\mathbf{r})$, can be regarded as an average density obtained by averaging the true density $\rho(\mathbf{r})$ over an appropriate local volume. It should be sufficiently smooth that the free energy can be calculated in local density approximation, i.e. we write

$$\mathscr{F}_{\text{hs}}[\rho] = \int d^3\mathbf{r} f_{\text{id}}(\rho(\mathbf{r})) + \int d^3\mathbf{r}\rho(\mathbf{r})\Delta\psi_{\text{hs}}(\bar{\rho}(\mathbf{r})), \tag{4}$$

where we have separated the ideal gas contribution, which is given exactly by the local density expression, and introduced $\Delta\psi_{\text{hs}}(\rho)$, the configurational part of the free energy per molecule

$$\Delta\psi_{\text{hs}}(\rho) = \frac{1}{\rho}(f_{\text{hs}}(\rho) - f_{\text{id}}(\rho)) \tag{5}$$

with

$$f_{\text{id}}(\rho) = k_{\text{B}}T\rho(\ln(\Lambda^3\rho) - 1). \tag{6}$$

$\Lambda = (h^2/2\pi m k_{\text{B}}T)^{1/2}$ is the thermal de Broglie wavelength of the molecule of mass m.

Our prescription for $\bar{\rho}$ is that developed by Tarazona [13]. The smoothed density is given by an average of $\rho(\mathbf{r})$ weighted by a suitable function w, which is

allowed to depend on $\bar{\rho}$:

$$\bar{\rho}(\mathbf{r}) = \int d^3\mathbf{r}'\rho(\mathbf{r}')w(|\,\mathbf{r} - \mathbf{r}'\,|;\ \bar{\rho}(\mathbf{r})). \tag{7}$$

This is an implicit equation for $\bar{\rho}$ in terms of ρ. The weight function w is specified by requiring the direct correlation function $c_{\mathrm{hs}}(r;\ \rho)$ of a uniform hard-sphere fluid, obtained by functional differentiation of (4), be close to $c_{\mathrm{hs}}^{\mathrm{py}}(r;\ \rho)$, obtained from the Percus–Yevick approximation, for a wide range of densities ρ. More precisely, it is assumed that w has a power series expansion

$$w(r;\ \rho) = w_0(r) + w_1(r)\rho + w_2(r)\rho^2 + \cdots \tag{8}$$

and the first two cofficients w_0 and w_1 are calculated by comparison with the virial expansion of $c_{\mathrm{hs}}(r;\ \rho)$, while the third, w_2, is obtained from an empirical fit to the Percus–Yevick results. Explicit expressions for w_i, $i = 0, 1, 2$ were derived in [13] and are listed in the Appendix of the present paper. In practice the expansion is truncated at the third term and (7) reduces to a quadratic equation for $\bar{\rho}(\mathbf{r})$:

$$\bar{\rho}(\mathbf{r}) = \bar{\rho}_0(\mathbf{r}) + \bar{\rho}_1(\mathbf{r})\bar{\rho}(\mathbf{r}) + \bar{\rho}_2(\mathbf{r})(\bar{\rho}(\mathbf{r}))^2 \tag{9}$$

with coefficients

$$\bar{\rho}_i(\mathbf{r}) = \int d^3\mathbf{r}'\rho(\mathbf{r}')w_i(|\,\mathbf{r} - \mathbf{r}'\,|) \quad i = 0, 1, 2. \tag{10}$$

depending on $\rho(\mathbf{r})$. The physical root of (9) is easily determined [13]. When the Carnahan and Starling expression [17]

$$\Delta\psi_{\mathrm{hs}}(\rho) = k_{\mathrm{B}}\,T\,\frac{\eta(4 - 3\eta)}{(1 - \eta)^2}, \tag{11}$$

with $\eta = \pi\rho\sigma^3/6$, is used the direct correlation functions are in good agreement with Percus–Yevick results even for reduced densities $\rho\sigma^3$ as high as 0·8 [13]. Unlike the Percus–Yevick result: $c_{\mathrm{hs}}^{\mathrm{py}}(r;\ \rho) = 0$, $r > \sigma$, this approximation exhibits a non-zero but rapidly decaying tail for $r > \sigma$, the hard-sphere diameter.

This completes the specification of the smoothed density free energy functional (SDA). Inserting (4) into (1) and differentiating w.r.t. $\rho(\mathbf{r})$ yields an equation for the equilibrium density that can be solved by a suitable iteration procedure [13]. The accuracy of the approximation was tested by comparing the density profiles and interfacial tensions for hard spheres ($\phi_{\mathrm{att}} = 0$) near a single hard wall with the corresponding results from computer simulation. There is good agreement for the full range of fluid densities, i.e. up to bulk densities as high as $\rho\sigma^3 = 0{\cdot}81$ [13]. We note, moreover, that in the SDA the density at contact, ρ_{w}, satisfies the exact rule $k_{\mathrm{B}}\,T\rho_{\mathrm{w}} = p$, the bulk pressure.

(*b*) *Two-dimensional limit of the three-dimensional density functional*

In treating the possible phase equilibria of a fluid confined between two parallel walls we are led to consider the situation that occurs when the wall

separation H becomes very small. Intuitively we might expect two dimensional phase equilibria to ensue when H is about one molecular diameter (or less). It is important then to enquire how well a theory designed to describe the thermodynamic and structural properties of a three-dimensional fluid can account for the same properties in a two-dimensional fluid. If the theory yields sensible results in this limit it is reasonable to suppose that it will provide a realistic description of fluids in very narrow slits.

Consider a three-dimensional density of the form

$$\rho(\mathbf{r}) = \rho^{(2D)}\delta(z). \tag{12}$$

Although this diverges at $z = 0$ it generates a finite two-dimensional uniform density

$$\rho^{(2D)} = \frac{1}{A}\int d^3\mathbf{r}\rho(\mathbf{r}),$$

where $A = \iint dxdy$ is the area in the x-y plane. The configurational part of the hard-sphere free energy functional

$$\Delta\mathscr{F}_{hs}[\rho] = \int d^3\mathbf{r}\rho(\mathbf{r})\Delta\psi_{hs}(\bar{\rho}(\mathbf{r}))$$

is then

$$\Delta\mathscr{F}_{hs} = A\rho^{(2D)}\Delta\psi_{hs}(\bar{\rho}(0))$$

with $\bar{\rho}(0) \equiv \bar{\rho}(z = 0)$. Thus the SDA yields an excess (over ideal gas) free-energy per molecule

$$\Delta\psi_{hs}^{(2D)}(\rho^{(2D)}) = \Delta\psi_{hs}(\bar{\rho}(0)). \tag{13}$$

It is this quantity that is appropriate to the two-dimensional fluid. The smoothed density $\bar{\rho}(0)$ is obtained from (9)

$$\bar{\rho}(0) = 2\bar{\rho}_0[1 - \bar{\rho}_1 + ((1 - \bar{\rho}_1)^2 - 4\bar{\rho}_2\bar{\rho}_0)^{1/2}]^{-1} \tag{14}$$

where

$$\bar{\rho}_i \equiv \bar{\rho}_i(0) = \rho^{(2D)}\iint dxdyw_i((x^2 + y^2 + z^2)^{1/2})_{z=0}, \quad (i = 0, 1, 2). \tag{15}$$

Using the w_i in the Appendix explicit formulae can be obtained for $\bar{\rho}_i$. The approximation for the excess free-energy of the hard-sphere fluid in the two-dimensional limit is, from (13) and (11),

$$\Delta\psi_{hs}^{(2D)}(\rho^{(2D)}) = k_B T\frac{\bar{\eta}(4 - 3\bar{\eta})}{(1 - \bar{\eta})^2}, \tag{16}$$

with $\bar{\eta} = \pi\bar{\rho}(0)\sigma^3/6$. We have compared the results obtained from (16) with those from scaled particle theory [18] for hard discs:

$$\Delta\psi_{hs}^{(2D)}(\rho^{2D}) = k_B T\left[\frac{\eta^{(2D)}}{1 - \eta^{(2D)}} - \ln(1 - \eta^{(2D)})\right], \tag{17}$$

with $\eta^{(2D)} = \pi\rho^{(2D)}\sigma^2/4$. Although the forms of these approximations appear completely different the numerical results agree to within 10% for reduced densities

$\rho^{(2D)}\sigma^2 \leqslant 0{\cdot}6$. For higher densities (16) overestimates the excess free energy. Similar remarks apply to the pressure

$$p_{hs}^{(2D)}(\rho^{(2D)}) = \rho^{(2D)}\left[\rho^{(2D)}\frac{d\Delta\psi_{hs}^{(2D)}}{d\rho^{(2D)}} + k_B T\right]. \tag{18}$$

We conclude that our three-dimensional theory provides an adequate description of the two-dimensional hard-disc fluid.

If we include the attractive tail of the pair-potential via (2) it is possible to calculate the critical points for both three and two-dimensional bulk fluids. We assume, for convenience, a Yukawa tail

$$\phi_{att}(r) = -\frac{\alpha\lambda^3 \exp(-\lambda r)}{4\pi\lambda r} \tag{19}$$

where α is a measure of the strength of the attractive forces and λ^{-1} is a measure of their range. In three dimensions $\int d^3\mathbf{r}\phi_{att}(\mathbf{r}) = -\alpha$ and the free energy density of the uniform fluid reduces to

$$f(\rho) = f_{hs}(\rho) - \alpha\rho^2/2.$$

This result is valid for *both* the LDA(3) and the SDA(4). Note that $\int d^3\mathbf{r}w(r;\rho) = 1$. The equation of state is

$$p(\rho) = p_{hs}(\rho) - \alpha\rho^2/2$$

with $p_{hs}(\rho) = \rho k_B T(1 + \eta + \eta^2 - \eta^3)/(1-\eta)^3$, the Carnahan and Starling result [17]. The critical density $\rho_c \equiv \rho_c^{(3D)}$ and temperature $T_c \equiv T_c^{(3D)}$ are then easily obtained [16]:

$$\rho_c\sigma^3 = 0{\cdot}249; \quad 11{\cdot}102k_B T_c\sigma^3 = \alpha. \tag{20}$$

In two dimensions the attractive tails contribute a term

$$\tfrac{1}{2}\rho^{(2D)2}\int d^2\mathbf{r}\phi_{att}(r) = -\frac{\lambda\alpha\rho^{(2D)2}}{4}$$

to the free energy density and the pressure. The hard-sphere contribution to the pressure follows from (18). Using the two-dimensional limit (16) we find

$$\rho_c^{(2D)}\sigma^2 = 0{\cdot}242; \quad 19{\cdot}77k_B T_c^{(2D)}\sigma^2 = \alpha\lambda \tag{21}$$

while the scaled particle result (17) gives

$$\rho_c^{(2D)}\sigma^2 = 0{\cdot}274; \quad 18{\cdot}35k_B T_c^{(2D)}\sigma^2 = \alpha\lambda. \tag{22}$$

The ratio of critical temperatures obtained from the SDA is

$$\frac{T_c^{(2D)}}{T_c} = 0{\cdot}5615\lambda\sigma. \tag{23}$$

In our calculations for slits we set $\lambda^{-1} = \sigma$. Then (23) implies that for $T < T_c^{(2D)} = 0{\cdot}56T_c$ it should be possible to find two-dimensional-like liquid–gas coexistence in very narrow slits, $H \to 0$. If $T > T_c^{(2D)}$ we should expect the line of coexistence to terminate at a larger value of H. We shall see that these predictions are confirmed by the results of our calculations. Note that in the LDA $\mathscr{F}_{hs}[\rho]$ is ill-defined for $\rho(z) = \rho^{(2D)}\delta(z)$ so the two-dimensional limit is not meaningful.

3. Application to three interfacial problems

In this section we report the results of calculations of several properties of fluids at different types of interface. The calculations are based on the SDA and the results are compared with those from the simpler LDA. This allows us to assess the importance of non-local contributions to the free-energy functional for a variety of problems.

(*a*) *Wetting behaviour at a single wall*

We have calculated the density profiles $\rho(z)$ and interfacial tensions γ for a fluid, described by the attractive pair potential (19), near a wall that exerts a wall–fluid potential

$$V_s(z) = \begin{cases} \infty, & z < 0, \\ -\varepsilon_w \exp(-\lambda z), & z > 0. \end{cases} \tag{24}$$

For a given well-depth $\varepsilon_w(>0)$, the fluid undergoes a wetting transition from partial wetting, contact angle $\theta > 0$, to complete wetting, $\theta = 0$, at a temperature $T_w < T_c$. θ is defined by Young's equation $\gamma_{wg} = \gamma_{wl} + \gamma_{lg} \cos\theta$, where the wall–gas tension γ_{wg}, wall–liquid tension γ_{wl} and liquid–gas tension γ_{lg} all refer to bulk coexistence. In the LDA the free-energy functional then corresponds to the model introduced by Sullivan [16]. This model exhibits a second-order wetting transition, i.e. the thickness of the adsorbed liquid film at the wall–gas interface diverges and $d(\cos\theta)/dT$ vanishes continuously as $T \to T_w$ along the bulk coexistence curve. Increasing ε_w lowers the wetting transition temperature T_w [16]. By making the range (λ^{-1}) of the wall potential larger than that of the attractive fluid–fluid potential it is possible to drive the transition first-order [19–21]. In this case the film thickness diverges and $d(\cos\theta)/dT$ vanishes discontinuously as $T \to T_w$ [22]. The purpose of our present calculations was to examine the effects of non-locality of the functional on the nature of the wetting transition. To this end we varied the product of the hard sphere diameter and the (common) inverse range λ of the potentials. In the limit $\sigma\lambda \to 0$ the interfacial tensions are the same as those obtained in the LDA of Sullivan [16]. For $\sigma\lambda > 0$ non-locality manifests itself.

Results for T_w as a function of $\sigma\lambda$ for several values of ε_w are plotted in figure 1. At $\sigma\lambda = 0$ we recover the results of Sullivan [16]. As $\sigma\lambda$ is increased the wetting temperature decreases slowly for weak wall potentials but more rapidly for stronger potentials. The transition remains second order for small $\sigma\lambda$ but becomes first order† at large $\sigma\lambda$. The stronger the wall potential (larger ε_w) the smaller is the value of $\sigma\lambda$ at which the cross-over occurs. Thus for $\varepsilon_w = 3k_B T_c$, a value appropriate to a fairly weak substrate, T_w falls from $0.82T_c$ at $\sigma\lambda = 0$ to $0{\cdot}55T_c$ at $\sigma\lambda = 0{\cdot}9$ and the transition is then first order. A similar reduction in T_w/T_c was found in the work of Freasier and Nordholm [23] and Meister and Kroll [14]. The effects of non-locality are clearly important in determining both the location and the order of the wetting transition. In a non-local treatment the fluid density near the wall is increased above that of the local density approximation. This enhancement can be interpreted as arising from an increase in the

† The method of locating the transition and ascertaining its order is described in [19].

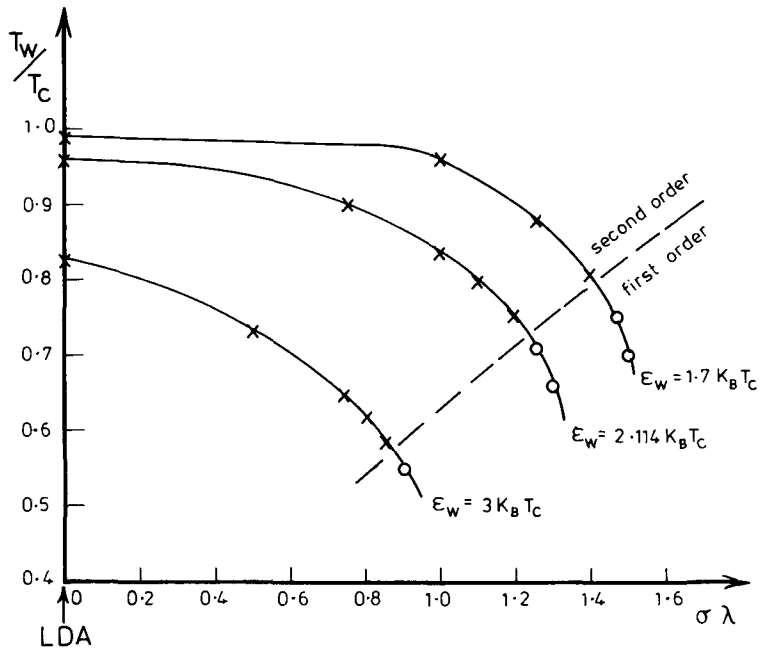

Figure 1. The wetting transition temperatures T_w calculated in the SDA for different strengths, ε_w, of the wall–fluid potential. $\sigma\lambda$ determines the range of the potential functions; $\sigma\lambda = 0$ corresponds to the LDA of Sullivan. The crosses denote second order and circles first order transitions.

effective strength of the attractive wall–fluid potential. Such a mechanism favours complete wetting, i.e. T_w is shifted to a lower temperature. The present theory is capable of describing solid–liquid and solid–gas coexistence as well as liquid–gas coexistence and the triple point temperature T_t, obtained from a procedure similar to that employed in earlier density functional calculations of freezing [24], is $\lesssim 0{\cdot}47 T_c$. The results shown in figure 1 indicate that the wetting transition will only occur above T_t for a reasonably ranged potential function ($\sigma\lambda \sim 1$, say) provided $\varepsilon_w \lesssim 3k_B T_c$. For a stronger attractive potentials we would expect to find complete wetting for all $T > T_t$.

Examples of the density profiles obtained from the SDA are shown in figure 2. These refer to a wall potential with $\varepsilon_w = 2{\cdot}114 k_B T_c$, a value appropriate to argon at a carbon-dioxide substrate [25], and $\sigma\lambda = 1$. The profiles correspond to the wall–gas interface at different temperatures but, in each case, at bulk coexistence. As T is increased one observes the growth of thicker liquid-like films near the wall. At the highest temperature, $T = 0{\cdot}835 T_c$, three distinct oscillations, corresponding to three closely packed 'liquid layers', followed by a relatively flat portion occur in $\rho(z)$. The wetting transition, which is second order in this system, takes place at a slightly higher temperature. We emphasize that the LDA, whilst also predicting a second-order transition (at $T_w \approx 0{\cdot}96 T_c$ for this wall-potential), yields monotonically decreasing density profiles with no ordering due to short-ranged correlations (packing) near the wall.

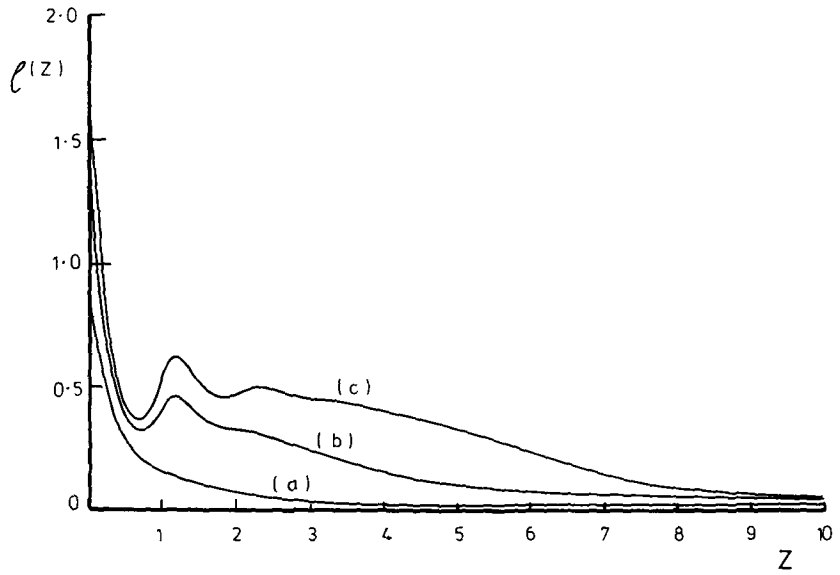

Figure 2. Density profiles for a wall–gas interface at bulk coexistence (*a*) $T = 0{\cdot}7T_c$, (*b*) $T = 0{\cdot}8T_c$ and (*c*) $T = 0{\cdot}835T_c$. The fluid undergoes a second order wetting transition at a temperature slightly higher than in (*c*). Reduced units $\sigma = \lambda^{-1} = 1$ are used.

(*b*) *Capillary evaporation in a slit with hard walls*

The second application is concerned with the phase equilibria of the Yukawa fluid described by (19), confined by two parallel hard walls. These exert a total potential

$$V(z) = \begin{cases} \infty, & z < 0 \quad \text{and} \quad z > H \\ 0, & 0 < z < H. \end{cases} \tag{25}$$

It is well known that for a *single* hard-wall the wall–liquid interface exhibits the phenomenon of complete drying ($\theta = \pi$) or wetting by gas. When the pressure, p, of the bulk liquid (far away from the wall) is reduced to its value at coexistence, p_{sat}, the density profile loses the oscillations that characterize the wall–liquid interface and in the limit $p \to p_{sat}$ a wetting layer of low-density gas intrudes between the wall and the liquid. Such behaviour has been found in computer simulations of Lennard-Jones fluids [26] and, more recently, in detailed simulations of a square-well fluid [27]. Earlier density functional calculations [13], based on a simplified version of the SDA, gave a satisfactory account of the erosion of oscillations and the growth of the gas layer—see also Meister and Kroll [14]. The purpose of the present calculations was to investigate the effects of confinement on a fluid that is in the complete drying regime.

It is assumed that the walls are unbounded in the x and y directions but the fluid is in contact with a reservoir at fixed T and μ. For a given wall separation H the fluid between the walls will adopt that density profile which minimizes the grand potential $\Omega(\mu, T, H)$. If H is large we expect the profile to be a superposition of the profiles at the individual walls. Thus for $\mu \gtrsim \mu_{sat}(p \gtrsim p_{sat})$ the profile should have the form sketched in figure 3(*a*), with most of the volume of

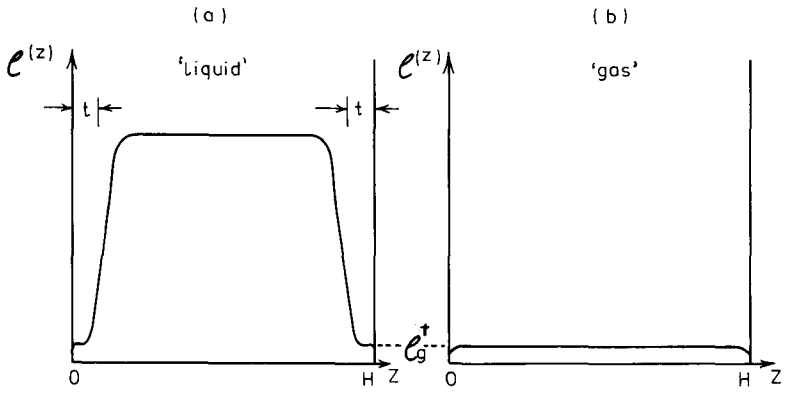

Figure 3. Density profiles (schematic) of a fluid confined in a slit with hard walls. (*a*) a 'liquid' configuration with wetting layers of gas of thickness t (*b*) a 'gas' configuration. These configurations coexist at a chemical potential $\mu > \mu_{sat}$. The wall separation $H \gg \sigma$.

the slit occupied by a 'liquid' whose density is similar to that of the bulk liquid at chemical potential μ. Thin layers of gas, with density ρ_g^+ corresponding to the metastable bulk gas at the same value of μ, can develop at the walls. For larger μ the profile exhibits oscillations and the gas layers disappear. As $\mu \to \mu_{sat}$, however, the gas layers thicken and at a single wall the thickness t increases as [8]

$$\lambda t \sim -\ln (2(\mu - \mu_{sat})/\alpha\rho_g), \tag{26}$$

where ρ_g is the density of the gas at bulk coexistence. In the confined fluid the formation of thick gas layers is in competition with capillary evaporation. As μ is decreased for fixed H, or H is decreased at fixed μ (T fixed), the fluid can undergo a first-order phase transition to a 'gas' state with a density profile similar to that sketched in figure 3(*b*). This transition corresponds to a shift of the bulk first-order transition, i.e. evaporation of liquid at $\mu > \mu_{sat}$. In the limits $H \to \infty$ and $\mu \to \mu_{sat}$ macroscopic arguments [4] show that capillary evaporation occurs in a complete drying regime when

$$p - p_g^+ = 2\gamma_{lg}/H \tag{27}$$

where p_g^+ is the pressure of the metastable gas at chemical potential μ. For bulk pressures $p(\mu)$ greater than the value predicted by (27) the 'liquid' configuration of figure 3(*a*) is stable, while for smaller pressures the 'gas' configuration of figure 3(*b*) is stable. The two distinct configurations coexist when $p(\mu)$ satisfies (27). Evidently (27) has the form of the Laplace result for the pressure difference across a convex cylindrical meniscus with mean radius of curvature H [4]. By calculating the grand potential of the inhomogeneous fluid using the density functional approach we were able to investigate the regime of validity of this macroscopic approximation.

The results of our calculations for the coexistence line at a fixed temperature $T = 0{\cdot}7T_c$ are shown in figure 4. We set $\sigma = \lambda^{-1} = 1$. There is very little difference between the results from the two different approximations for $H \gtrsim 10$. In this range the density profiles from the SDA for 'liquid' configurations near capillary coexistence are quite similar to those obtained from the LDA. Since the

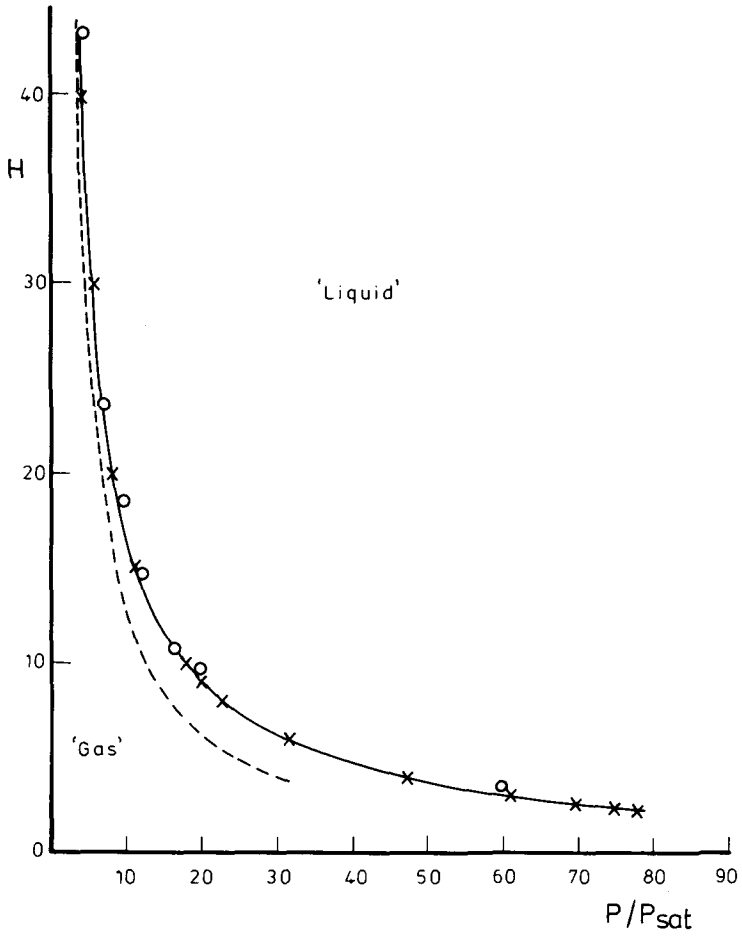

Figure 4. Capillary coexistence line for a fluid confined in a slit with hard walls. The wall separation H is measured in reduced units $\sigma = \lambda^{-1} = 1$. p is the pressure of the bulk liquid at chemical potential $\mu > \mu_{sat}$. The crosses joined by a solid line are the results of the SDA, the circles are results of the LDA and the dashed line is the Laplace result (27)—see text. $T = 0{\cdot}7T_c$.

reduced liquid–gas surface tensions $\gamma^*_{lg} \equiv \gamma_{lg}\sigma^2/k_B T_c$ differ only slightly (0·638 in SDA and 0·646 in LDA) we have plotted only one curve for the Laplace result (27). The latter is an adequate approximation for $H \gtrsim 40$ but underestimates the evaporation pressure at smaller separations†. Moreover it fails to account for the capillary critical point that is predicted by the density functional theories. For $H \lesssim 2$ in the SDA and $H \lesssim 3$ in the LDA there is no capillary evaporation.

Although wetting layers of gas do develop between the walls and the liquid these are very thin even for separations as large as $H = 40$. The maximum thickness that can be observed in a stable 'liquid' configuration is that which occurs at

† Equation (27) is only meaningful when there is a bulk gas at the same μ, i.e. in the metastable region. For $p/p_{sat} \gtrsim 33$ there is no metastable gas.

capillary coexistence. An estimate can be obtained by combining (26) and (27)

$$\lambda t \sim \ln\,(H\alpha\rho_g(\rho_l - \rho_g)/4\gamma_{lg}) \tag{28}$$

where we have expanded the pressures about p_{sat} and used $(\partial p/\partial\mu) = \rho$. ρ_l is the density of the liquid at bulk coexistence. For $H = 40$ (28) predicts $t \sim 0.7$. This agrees to within a factor of two with the maximum thickness obtained from our calculations. Our results suggest that in grand canonical simulations of liquids confined by hard-walls capillary evaporation to a dilute 'gas' configuration will occur before thick gas films can develop. (Simulations are presently restricted to $H \ll 40$ molecular diameters.) Henderson and van Swol did observe rather thick gas films with $H = 32\sigma$ but their simulations were for a fixed number of molecules [27]. Capillary evaporation does not occur in that ensemble and it is inappropriate to compare our results directly with theirs. In the analysis of their results Henderson and van Swol ignore the effects of finite H and assume their results are, effectively, those that would pertain to a single wall. Further work is required to assess the validity of their assumption.

(*c*) *Capillary condensation in slits and cylinders with attractive walls*

We turn now to the phase equilibria of the same Yukawa fluid confined in (*a*) a slit whose walls exert a total potential

$$\begin{aligned} V(z) &= V_s(z) + V_s(H - z) \\ &= \begin{cases} \infty, & z < 0 \quad \text{and} \quad z > H, \\ -\varepsilon_w[\exp\,(-\lambda z) + \exp\,(-\lambda(H - z))], & 0 < z < H \end{cases} \end{aligned} \tag{29}$$

and (*b*) a cylinder of interior radius R_c whose wall exerts a potential

$$V(R) = \begin{cases} \infty, & R > R_c \\ -2\varepsilon_w \lambda R_c K_1(\lambda R_c) I_0(\lambda R), & R < R_c \end{cases}, \tag{30}$$

where R is the radial distance from the axis of the (infinitely long) cylinder and I_0 and K_1 are modified Bessel functions. The potential (30) is that which is obtained when a molecule in the fluid interacts with a molecule in the wall via a Yukawa pairwise potential $\alpha - \exp\,(-\lambda r)/r$. In the limits $R_c \to \infty$ and $R \to \infty\, V(R) \to -\varepsilon_w \exp\,(-\lambda z)$, provided $z = |R_c - R| \ll R_c$. Equations (29) and (30) were employed in our earlier calculations [5] based on the LDA. The aim of the present work was to investigate whether or not the incorporation of non-local effects would alter significantly the picture of phase-equilibria that emerged from the earlier studies [4, 5]. We focused attention on narrow capillaries since it is for these that we expect packing considerations to be most important. Moreover we specialized to those (low) temperatures where two-dimensional-like behaviour might occur for a realistic treatment of the confined fluid but would not occur in the LDA.

Calculations were performed in the SDA with the strength parameter $\varepsilon_w = 2{\cdot}114 k_B T_c$ and $\sigma = \lambda^{-1} = 1$. This particular model, in slit geometry, was studied in detail in earlier papers [4, 28] using the LDA. It was found that for $T > T_s$ capillary condensation from a dilute 'gas' configuration to a dense 'liquid' configuration occurred as μ increased towards μ_{sat}. T_s is the temperature at which $\cos\theta = 0$; for $T < T_s$ $\cos\theta$ is negative. In the LDA $T_s \approx 0{\cdot}57 T_c$. The pressure, p, at which the first order transition occurred was compared with that from the

Laplace equation

$$p - p_l^+ = 2\gamma_{lg} \cos \theta / H \tag{31}$$

where p_l^+ is the pressure of the metastable liquid at the same value of μ. Equation (31) was reasonably accurate for $H \gtrsim 10$ and temperatures $T < T_w (\approx 0{\cdot}96 T_c$ in LDA). For $T > T_w$ wetting films of liquid develop at the walls and produce substantial corrections to (31). The lines of capillary coexistence, H versus μ or p at fixed T, were predicted to terminate at critical points for small values of H. SDA results for $T = 0{\cdot}6 T_c$ and $0{\cdot}5 T_c$ are presented below. Both temperatures lie below $T_w \approx 0{\cdot}835 T_c$ (see § 3(*a*)); the first is above, while the second is below the two-dimensional critical temperature $T_c^{(2D)} = 0{\cdot}56 T_c$ derived in § 2(*b*).

In figure 5 we plot the capillary coexistence curves for slits and cylinders at $T = 0{\cdot}6 T_c$. Note that the degree of undersaturation is given by the ratio ρ_b/ρ_g, where ρ_b is the bulk gas density at chemical potential $\mu (< \mu_{sat})$ and ρ_g is its density at coexistence. For H or $R_c \gtrsim 2$ the results for both slits and cylinders agree

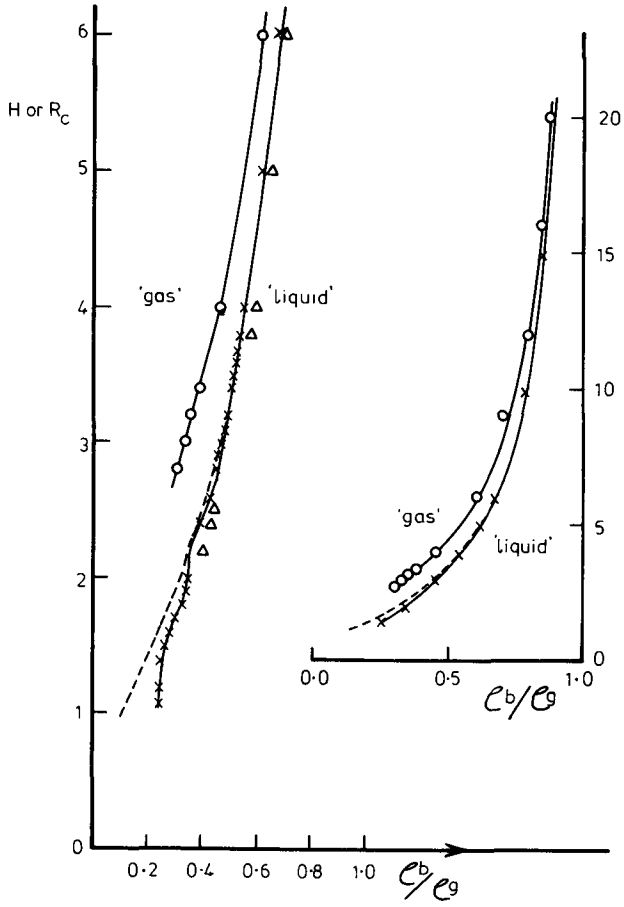

Figure 5. Capillary coexistence lines for fluids confined in slits of width H and cylinders of radius R_c at $T = 0{\cdot}6 T_c$. The crosses joined by a solid line are the results for slits and the triangles are the results for cylinders in the SDA. The dashed line is the Laplace result (31). The circles joined by a solid line are the results for slits in the LDA—see text.

remarkably well with the Laplace estimate (31). The latter yields the same estimate in both cases—H being replaced by R_c for cylinders. The condensation pressure is only slightly larger in cylinders than in slits and this is consistent with LDA results for $T < T_w$ [5]. Near $H = 1$, $H = 2$ and, to a lesser extent, $H = 3$ the capillary coexistence line calculated for slits exhibits oscillations. These are associated with packing effects and are much more pronounced at the lower temperature. We were unable to find coexistence for $H < 1$ and we conclude that the coexistence line ends in a capillary critical point near $H = 1$.

Also shown in figure 5 are the results of calculations for slits based on the LDA for the same temperature but a different value of ε_w. If we employed the same value for ε_w the contact angle would be much larger in the LDA since the wetting transition occurs at a higher temperature. Thus $\gamma_{lg} \cos \theta$ would be significantly smaller in the LDA than in the SDA at the same temperature, forcing the condensation pressure to higher values for a given separation. To avoid this difficulty and effect a fairer comparison between the results of the two approximations, we increased ε_w to $2{\cdot}829 k_B T_c$, the value for which $\gamma_{lg} \cos \theta = \gamma_{wg} - \gamma_{wl}$ is the same as in the SDA. Both approximations now yield the same asymptotic (Laplace) result as $H \to \infty$. The LDA results are in close agreement with those of the SDA for $H \gtrsim 12$ but for smaller separations the condensation pressure is underestimated. Of course the coexistence line does not show oscillatory character and it terminates in a capillary critical point at $H > 2$. Somewhat surprisingly, we find that the LDA results are much further removed from the Lapace estimate than the SDA results.

The results just described show no features that could be ascribed to two-dimensional-like phase equilibria. As expected the situation is quite different for $T = 0{\cdot}5 T_c < T_c^{(2D)}$. Before presenting the numerical results it is instructive to return to the problem, raised earlier, of very narrow slits. For H slightly greater than 1 we expect the density profile of a 'liquid' configuration to take the form sketched in figure 6(*a*). This corresponds to two highly localized layers and these are drawn schematically in figure 6(*b*). If H is reduced below 1 the liquid can develop only a single layer (figure 6(*d*)) and the density profile resembles that in figure 6(*c*). As H is reduced even further the liquid becomes more two-dimensional like; the two-dimensional limit corresponds to $H \to 0$. At $T = 0{\cdot}5 T_c = 0{\cdot}83 T_c^{(2D)}$ the reduced densities of coexisting *two dimensional* liquid and gas are 0·45 and 0·08, respectively, in the SDA. If we define an effective two-dimensional density $\rho_{eff}^{(2D)} = \int_0^H dz \rho(z)$ for the three-dimensional fluid in the slit we would expect to find for sufficiently small H, that condensation occurs between 'liquid' and 'gas' configurations that have densities $\rho_{eff}^{(2D)}$ similar to the values quoted above. Our calculations showed that this was indeed the case for $H < 0{\cdot}8$. Moreover, for $0{\cdot}1 \lesssim H \lesssim 0{\cdot}7$, the effective densities were almost independent of H; the 'liquid' always having a density greater than 0·45 and the 'gas' a density less than 0·08. For these small separations $\rho(z)$ is almost constant and varies as $\rho_{eff}^{(2D)}/H$. We believe that this is strong evidence for two-dimensional like condensation. For very small H, i.e. $H \lesssim 0{\cdot}2$, the capillary coexistence line (see figure 7) bends towards larger pressures. This behaviour can be attributed to the ideal gas term in the chemical potential. The chemical potential of the three-dimensional fluid can be written as

$$\mu(\rho) = \mu_{id}(\rho) + \Delta\mu_{hs}(\rho) - \alpha\rho$$

where $\mu_{id}(\rho) = k_B T \ln (\Lambda^3 \rho)$ and $\Delta\mu_{hs}$ is the non-ideal (configurational) part of the hard-sphere chemical potential. In the limit $H \to 0$ we can approximate ρ by $\rho_{eff}^{(2D)}/H$ so that

$$\mu_{id}(\rho) \approx k_B T \ln (\Lambda^2 \rho_{eff}^{(2D)}) + k_B T \ln (\Lambda/H)$$

$$= \mu_{id}^{(2D)}(\rho_{eff}^{(2D)}) + k_B T \ln (\Lambda/H).$$

Thus if coexistence occurs in the two-dimensional fluid for a given $T < T_c^{(2D)}$ at some density $\rho_{eff}^{(2D)}$ (gas or liquid) the corresponding ideal gas chemical potential of the three-dimensional fluid is shifted by an amount $k_B T \ln (\Lambda/H)$. Since the latter quantity diverges as $H \to 0$ this implies that the coexistence, referred to the three-dimensional system, is driven towards $\rho_b = \infty$. Consequently for $T < T_c^{(2D)}$ there is no capillary critical point and the coexistence line extends to $H = 0$ as $\rho_b \to \infty$.

The packing effects alluded to in figure 6 produce the oscillation of the coexistence line near $H = 1$. Similar considerations apply near $H = 2$. The insets to figure 7 show that oscillations are more pronounced in slits than in cylinders so we concentrate on the former. As H is increased at fixed undersaturation, from about 0·9 to 1·1, the density of the liquid at the walls, $\rho(0) = \rho(H)$, increases

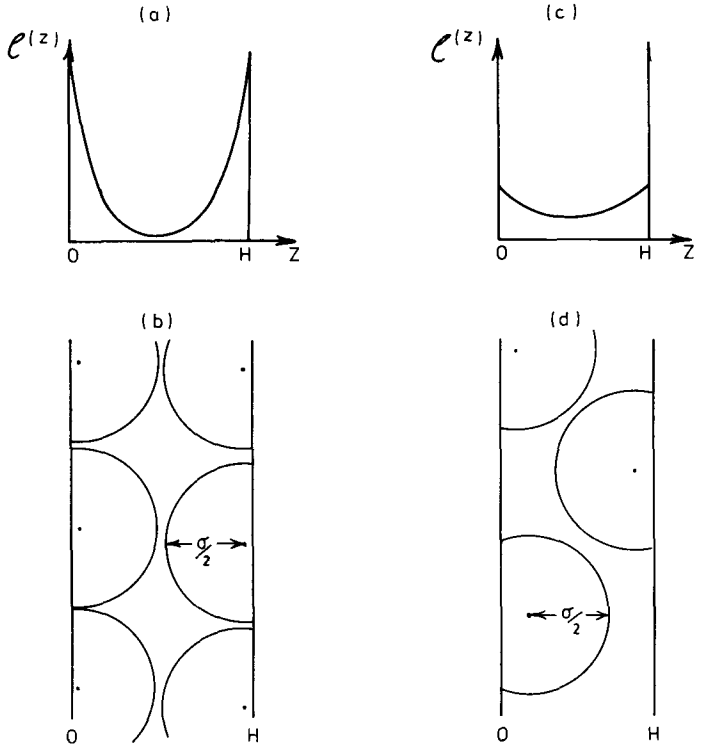

Figure 6. Effects of packing on the density profile $\rho(z)$ of a liquid confined in a narrow slit. In (*a*) and (*b*) the wall separation H is slightly greater than the hard-sphere diameter σ and two well-defined layers develop. In (*c*) and (*d*) $H < \sigma$ and a single loosely-packed layer develops. As $H \to 0$ the nuclei • become restricted to a single plane.

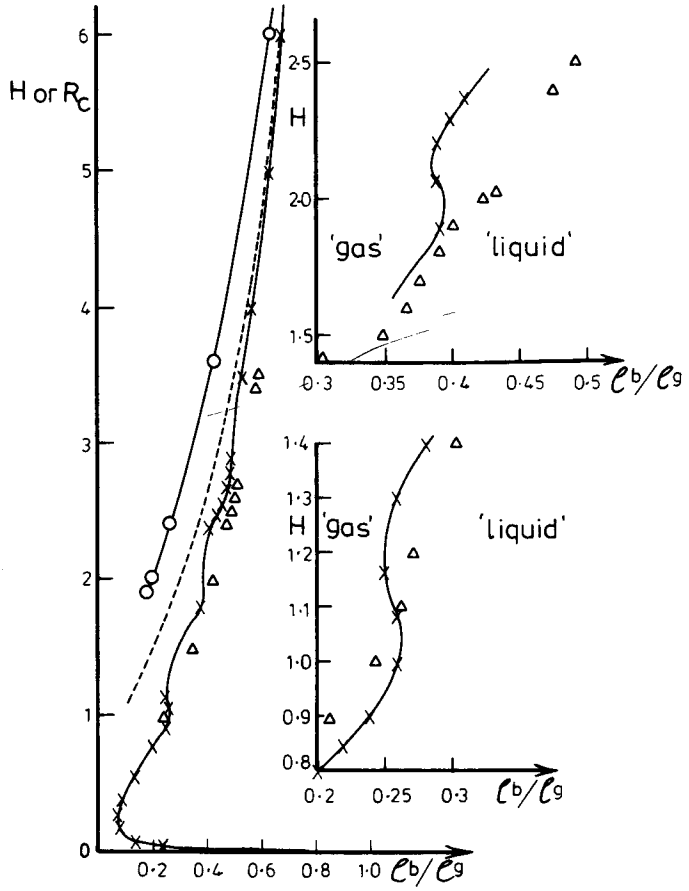

Figure 7. As in figure 5 but now for $T = 0{\cdot}5T_c$. Note that the coexistence line in the LDA (circles) terminates in a capillary critical point near $H = 1{\cdot}9$ whereas it continues to $H = 0$ in the SDA (crosses). The triangles denote the SDA results for cylinders.

significantly while the density at mid-point, $\rho(H/2)$, decreases. The effect is especially pronounced for values of $\rho_b/\rho_g \approx 0{\cdot}25$ (figure 8) where $\rho(0)$ increases by a factor of 3·5 and $\rho(H/2)$ decreases by a factor of 2·5 between $H = 0{\cdot}95$ and $H = 1{\cdot}1$. (Note that the 'liquid' is metastable w.r.t. 'gas' for $H > 0{\cdot}93$ at this undersaturation). It is tempting to speculate that a first-order phase transition might occur between the one-layer and two-layer 'liquid' configurations sketched in figure 6. This would be characterized by discontinuities in $\rho(0)$ and $\rho(H/2)$, plotted as a function of H. We did not observe such discontinuities in these calculations—the metastable liquid branch terminates before loops can be generated in $\rho(H/2)$, say.

The rapid change in the structure of the 'liquid' near $H = 1$ generates an oscillation in the surface excess grand potential [4] $\gamma(H) = (\Omega/A + pH)/2$. $\gamma(H)$ is plotted in figure 9 for both 'liquid' and 'gas' configurations at several undersaturations. $\gamma_g(H)$ varies monotonically with H and is rather insensitive to the undersaturation. The genesis of the capillary coexistence line shown in figure 7 is

now apparent. On increasing H at fixed ρ_b/ρ_g (i.e. bulk pressure or chemical potential) the fluid can undergo a single transition from 'liquid' to 'gas', as in figure 9(*a*) and 9(*b*) or three transitions from 'liquid' to 'gas' to 'liquid' to 'gas', as in figure 9(*c*). Equivalent behaviour occurs for higher pressures near $H = 2$. On reducing the temperature still further the oscillations in the capillary coexistence lines become more pronounced and extend to larger H.

From figure 7 it can be seen that although on an unexpanded scale the coexistence line calculated for cylinders lies very close to that for slits there are quantitative differences at small H or R_c, when packing considerations become crucial. The SDA results for both cylinders and slits lie very close to the Laplace result (31) for H or $R_c \gtrsim 6$. The LDA results shown in figure 7 were obtained by the same procedure that was employed at the higher temperature, i.e. ε_w was increased (to $3{\cdot}005 k_B T_c$) so that the Laplace result would be the same as that in the SDA. As was the case at the lower temperature the LDA results predict smaller condensation pressures than the SDA at small H. The LDA coexistence line terminates in a capillary critical point at $H \sim 1{\cdot}9$. This is in sharp contrast to the SDA result described above. That the LDA should always predict a critical point at some non-zero H is easily understood by reference to the slab approximation employed in our earlier paper [4]. Assuming the profiles $\rho(z)$ are constant throughout the slit one finds [4] in the LDA that the capillary critical

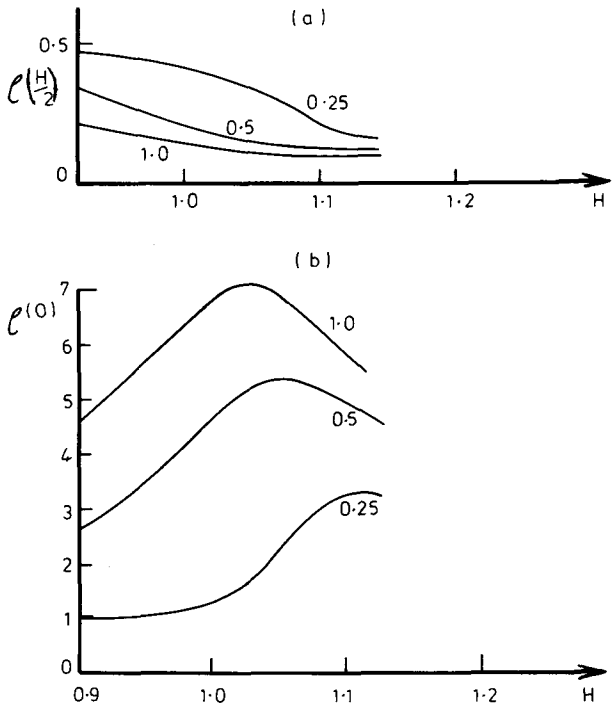

Figure 8. (*a*) The density at mid-point for 'liquid' configurations at $T = 0{\cdot}5 T_c$ (in reduced units) for three values of the undersaturation ratio ρ_b/ρ_g. (*b*) The density at the walls.

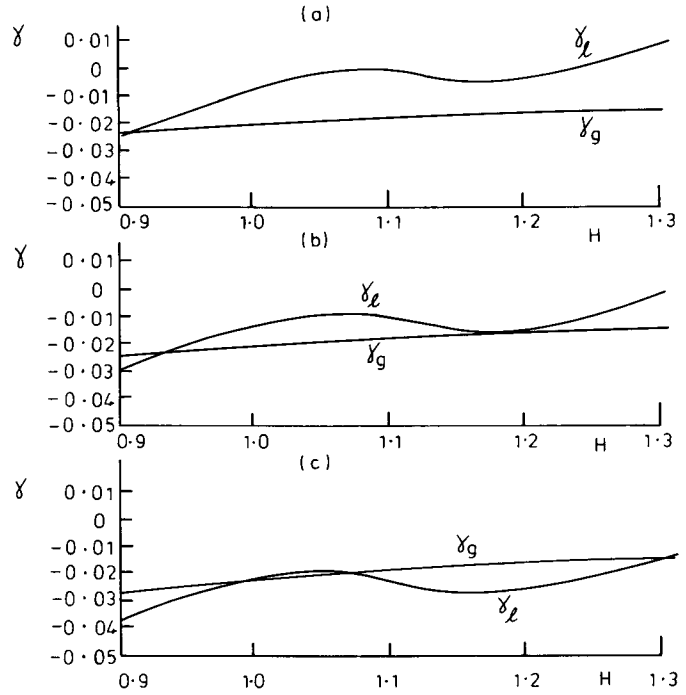

Figure 9. The surface excess grand potential γ for 'liquid' (γ_l) and 'gas' (γ_g) configurations at $T = 0{\cdot}5T_c$ as a function of wall separation H (in reduced units). (*a*) $\rho_b/\rho_g = 0{\cdot}24$, (*b*) $\rho_b/\rho_g = 0.25$ and (*c*) $\rho_b/\rho_g = 0{\cdot}26$.

temperature is given by

$$\frac{T_c^{cap}}{T_c} = 1 - (1 - \exp(-\lambda H))/\lambda H.$$

This approximation is reasonably accurate for small H. In the limit $H \to 0 T_c^{cap} \to 0$, i.e. there is no capillary coexistence.

Finally in figures 10 and 11 we give some examples of the density profiles calculated in the SDA. Figure 10 illustrates the pronounced layered structure that develops for a confined liquid in a narrow slit ($H = 4$). Five well-defined layers are present. We recall that in the LDA the density profile decreases monotonically [4] from the walls to the mid-point. In figure 11 we compare profiles for slits with those for cylinders. For $H = R_c = 2{\cdot}4$ the profiles are very similar. The cylinder contains a central 'chain' of molecules surrounded by two well-defined concentric annuli. Packing in the cylinder produces a central density $\rho(R = 0)$ that is even higher than that at the wall, $\rho(R_c)$. For $H = R_c = 2{\cdot}0$, however, the situation changes completely. The slit contains three well-defined layers of molecules while the packing in the cylinder is much looser with a well-defined annulus next to the wall and a smeared-out annulus located around $R = 0{\cdot}8$. Evidently packing effects are rather subtle.

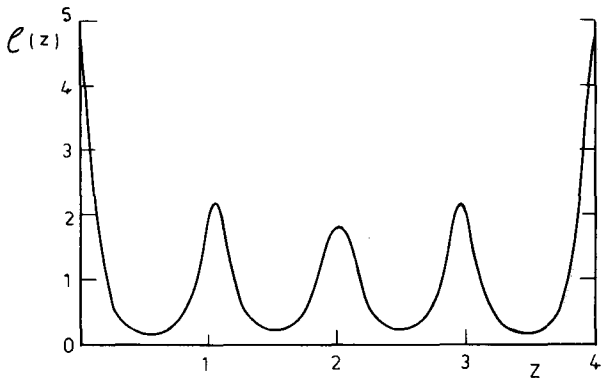

Figure 10. The density profile for a liquid confined in a slit with $H = 4$ ($T = 0{\cdot}5T_c$; $\rho_b/\rho_g = 0{\cdot}57$; $\sigma = \lambda^{-1} = 1$.)

4. Final remarks

Our comparison of results from the SDA and the LDA indicates that the incorporation of non-local contributions to the free energy functional can have important qualitative as well as quantitative consequences for the phase equilibria of non-uniform fluids.

In the case of a single attractive wall we have found that the inclusion of non-locality drives the wetting transition temperature T_w to lower values and tends to make the transition first-order. It is likely that T_w will depend sensitively on the details of the potential functions *and* the theory that it used to calculate it [29]. Moreover it is clear that in a partial wetting situation ($T < T_w$) the contact angle $\theta(T)$ will depend strongly on the choice of theory; the LDA probably underestimates cos θ for a given temperature and potential.

For the problem of capillary evaporation of a fluid between hard walls the LDA results are rather close to those of the SDA. This might have been anticipated since for $H \gtrsim 8$ the density profiles of 'liquid' do not exhibit pronounced oscillations for states close to capillary coexistence. Comparison with the results of simulation, i.e. grand canonical Monte Carlo, should be most valuable for this case. However, one should first ensure that the fluid has the same liquid-gas

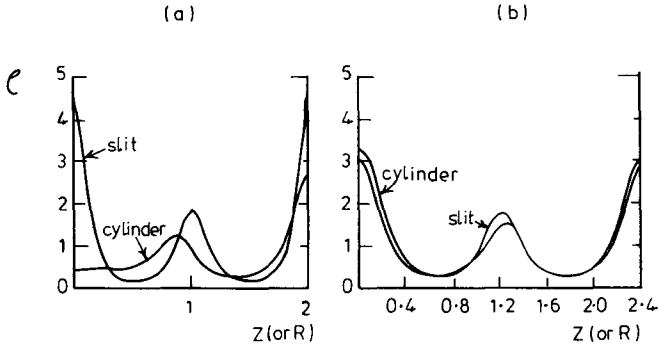

Figure 11. The density profiles for liquids confined in slits and cylinders ($T = 0{\cdot}5T_c$; $\rho_b/\rho_g = 0{\cdot}5$; $\sigma = \lambda^{-1} = 1$) (*a*) $H = R_c = 2$ and (*b*) $H = R_c = 2{\cdot}4$.

surface tension γ_{lg}, at the given T/T_c, in theory and simulation before comparing the capillary coexistence lines.

Several features of our results for capillary condensation warrant further comment. A striking feature is the close agreement between the SDA results for slits and cylinders with the results of the macroscopic Laplace equation when H or $R_c \gtrsim 5$ molecular diameters. We do not have a convincing explanation of why the macroscopic result should remain accurate for such small pores when $T < T_w$. The packing and hence the density profiles are certainly very different between cylinders and slits for such sizes but this does not appear to have a dramatic effect on the phase equilibria—see figures 5 and 7. It is only for H or $R_c \lesssim 3$ diameters that packing effects have a major influence on the shape of the capillary coexistence curve. Although the LDA omits all aspects of packing it still provides a reasonable zeroth-order description of the coexistence curve—provided the relevant parameter of the wall–fluid potential is chosen in such a way that $\gamma_{lg} \cos \theta$ is the same as in the SDA. The need for making this identification follows from our discussion of the single wall results; the local ordering at the wall increases $\cos \theta$. In other words we find that the contact angle is still a relevant parameter for narrow pores.

The LDA fails to account for two-dimensional-like phase equilibria. Thus it predicts capillary critical points for $T < T_c^{(2D)}$, whereas the SDA predicts, correctly, that the coexistence line should continue to $H = 0$. In this context it is instructive to note that the present SDA results have features in common with those obtained from the mean-field treatment of a nearest-neighbour lattice gas confined between two parallel walls [30]. The two-dimensional limit then corresponds to a single layer of lattice sites ($N = 1$), and $T_c(N = 1) \equiv T_c^{(2D)} = 0{\cdot}5T_c$ for the h.c.p. lattice in mean-field-approximation. Thus for $T < 0{\cdot}5T_c$ the capillary coexistence line extends to $N = 1$ whereas for $T > 0{\cdot}5T_c$ it terminates at some larger value of N. For $T < T_w$ the analogue of the Laplace equation (31) remains accurate down to $N \approx 8$ but the shape of the coexistence line for small N depends markedly on the form assumed for the wall–fluid potential [30].

The LDA also fails to describe the oscillations that develop in the SDA coexistence line for H or $R_c \lesssim 3$. As explained earlier these are associated with oscillations in $\gamma_l(H)$ which arise, in turn, from packing considerations in the 'liquid' configuration. It is important to recognize that $\gamma_l(H)$ decreases from its local maximum to its neighbouring local minimum in a distance of about 0·1 diameters in the neighbourhood of $H = 1$—see figure 9. This produces a solvation force per unit area $f(H) = -2(\partial\gamma/\partial H)_{\mu, T}$ that has zeroes near $H = 1{\cdot}05$ and $1{\cdot}15$. Now it is well-known [31] that in dense liquids (in the one-phase region) $f(H)$ usually oscillates with a period of 1 diameter for $H \gtrsim 2$. The SDA reproduces such behaviour [7]. The effect we are observing on the liquid branch for $\mu \ll \mu_{sat}$ and $H \sim 1$ is somewhat different from that observed in dense liquids at larger H. Further investigation of the solvation forces might well provide a better understanding of the effects of packing and layer formation on phase equilibria.

We have not addressed ourselves to the problem of capillary condensation when $T > T_w$, so that the liquid wets the walls completely. Under these circumstances we do not expect the results of the SDA to be substantially different from those of the LDA—provided $\gamma_{lg}(T)$ is the same so that both approximations yield the same Laplace limit. The capillary critical points might occur at smaller separations H than those calculated in the LDA [4, 5].

In conclusion we have demonstrated that the SDA is a versatile theory for fluid interfaces which is especially well-suited to the determination of phase equilibria. Although the simpler LDA is inferior in several aspects it provides an excellent starting point for understanding what possible phase transitions and related phenomena might occur in interfacial problems.

This research was supported by CAICYT (Spain) and SERC (U.K.). We are grateful to the British Council and the Spanish Ministry of Education for an Acciones Integradas grant which supported our collaboration.

Appendix

The weight function (8) used in this paper has coefficients

$$w_0(r) = \begin{cases} \dfrac{3}{4\pi\sigma^3}, & r < \sigma, \\ 0, & r > \sigma, \end{cases} \tag{A 1 a}$$

$$w_1(r) = \begin{cases} 0{\cdot}475 - 0{\cdot}648\left(\dfrac{r}{\sigma}\right) + 0{\cdot}113\left(\dfrac{r}{\sigma}\right)^2, & r < \sigma \\ 0{\cdot}288\left(\dfrac{\sigma}{r}\right) - 0{\cdot}924 + 0{\cdot}764\left(\dfrac{r}{\sigma}\right) - 0{\cdot}187\left(\dfrac{r}{\sigma}\right)^2, & \sigma < r < 2\sigma \\ 0 & r > 2\sigma, \end{cases} \tag{A 1 b}$$

and

$$w_2(r) = \begin{cases} \dfrac{5\pi\sigma^3}{144}\left(6 - 12\left(\dfrac{r}{\sigma}\right) + 5\left(\dfrac{r}{\sigma}\right)^2\right), & r < \sigma, \\ 0, & r > \sigma. \end{cases} \tag{A 1 c}$$

These satisfy $\int d^3\mathbf{r} w_0(r) = 1$ and $\int d^3\mathbf{r} w_i(r) = 0$ for $i = 1, 2$ so that $\int d^3\mathbf{r} w(\mathrm{r}; \rho) = 1$ for all ρ. Equation (A 1 *b*) is a simplified version of the fit to $w_1(r)$ given earlier [13]. Note that in [13] *and* its erratum the formulae for $w_1(r)$ and $w_2(r)$ are incorrect; factors of $\pi/6$ are missing. The correct formulae were employed in the calculations described in [13].

References

[1] Sullivan, D. E., and Stell, G., 1978, *J. chem. Phys.*, **69**, 5450.
[2] Evans, R., Tarazona, P., and Marini Bettolo Marconi, U., 1983, *Molec. Phys.*, **50**, 993.
[3] See, e.g., the review by Sullivan, D. E., and Telo da Gama, M. M., 1986, *Fluid Interfacial Phenomena*, edited by C. A. Croxton (Wiley), p. 45.
[4] Evans, R., Marini Bettolo Marconi, U., and Tarazona, P., 1986, *J. chem. Phys.*, **84**, 2376.
[5] Evans, R., Marini Bettolo Marconi, U., and Tarazona, P., 1986, *J. chem. Soc. Faraday Trans. II*, **82**, 1763.
[6] Evans, R., 1979, *Adv. Phys.*, **28**, 143.
[7] An exception is the paper of Freasier, B. C., and Nordholm, S., 1983, *J. chem. Phys.*, **79**, 4431, who used a non-local density functional theory.
[8] Tarazona, P., and Evans, R., 1982, *Molec. Phys.*, **47**, 1033.

[9] EVANS, R., and MARINI BETTOLO MARCONI, U., 1985, *Phys. Rev.* A, **32,** 3817.
[10] PETERSON, B. K., WALTON, J. P. B. R., and GUBBINS, K. E., 1986, *J. chem. Soc. Faraday Trans. II*, **82** 1788.
[11] NORDHOLM, S., JOHNSTON, M., and FREASIER, B. C., 1980, *Aust. J. Chem.*, **33,** 2139; JOHNSON, M., and NORDHOLM, S., 1981, *J. chem. Phys.*, **75,** 1953.
[12] TARAZONA, P., and EVANS, R., 1984, *Molec. Phys.*, **52,** 847.
[13] TARAZONA, P., 1985, *Phys. Rev.* A, **31,** 2672; 1985, *Ibid.*, **32,** 3148 (erratum).
[14] MEISTER, T. F., and KROLL, D. M., 1985, *Phys. Rev.* A, **31,** 4055.
[15] CURTIN, W. A., and ASHCROFT, N. W., 1985, *Phys. Rev.* A, **32,** 2909.
[16] SULLIVAN, D. E., 1979, *Phys. Rev.* B, **20,** 3991. SULLIVAN, D. E., 1981, *J. chem. Phys.*, **74,** 2604.
[17] CARNAHAN, N. F., and STARLING, K. E., 1969, *J. chem. Phys.*, **51,** 635.
[18] HELFAND, E., FRISCH, H. L., and LEBOWITZ, J. L., 1961, *J. chem. Phys.*, **34,** 1037.
[19] TARAZONA, P., and EVANS, R., 1983, *Molec. Phys.*, **48,** 799.
[20] TELETZKE, G. F., SCRIVEN, L. E., and DAVIS, H. T., 1983, *J. chem. Phys.*, **78,** 1431.
[21] HAUGE, E. H., and SCHICK, M., 1983, *Phys. Rev.* B., **27,** 4288.
[22] A wetting transition of this type was obtained first by Cahn, J. W., 1977, *J. chem. Phys.*, **66,** 3667. EBNER, C., and SAAM, W. F., 1977, *Phys. Rev. Lett.*, **38,** 1486.
[23] FREASIER, B. C., and NORDHOLM, S., 1985, *Molec. Phys.*, **54,** 33.
[24] TARAZONA, P., 1984, *Molec. Phys.*, **52,** 81.
[25] See [16]. It should be remarked that this model, which is much beloved of theorists, is hardly appropriate to the real system. Apparently solid CO_2 dissolves in argon!
[26] ABRAHAM, F. F., 1978, *J. chem. Phys.*, **68,** 3713. SULLIVAN, D. E., LEVESQUE, D., and WEISS, J. J., 1980, *J. chem. Phys.*, **72,** 1170.
[27] HENDERSON, J. R., and VAN SWOL, F., 1985, *Molec. Phys.*, **56,** 1313.
[28] EVANS, R., and TARAZONA, P., 1984, *Phys. Rev. Lett.*, **52,** 557.
[29] The SDA has been used to investigate the wetting transition for a Lennard-Jones 12-6 fluid near a Lennard-Jones 9-3 wall and the results are close to those obtained from an integral equation theory—see BRUNO, E., CACCAMO, C., and TARAZONA, P., 1986, *Phys. Rev.* A, **34,** 2536; 1987, *Ibid.* (to appear).
[30] BRUNO, E., MARINI BETTOLO MARCONI, U., and EVANS, R., 1986, *Physica* A (to appear).
[31] LANE, J. E., and SPURLING, T. H., 1980, *Aust. J. Chem.*, **33,** 231. SNOOK, I. K., and VAN MEGEN, W., 1980, *J. chem. Phys.*, **72,** 2907. MAGDA, J. J., TIRRELL, M., and DAVIS, H. T., 1985, *J. chem. Phys.*, **83,** 1888.